ACS OMEGA

Article

http://pubs.acs.org/journal/acsodf

Water Adsorption and Insertion in MOF-5

Yang Ming,[†,#] Nitin Kumar,[‡] and Donald J. Siegel[*,‡,§,∥,⊥]

[†]Department of Physics, University of Michigan, 1440 Randall Laboratory, 450 Church Street, Ann Arbor, Michigan 48109-1040, United States

[‡]Mechanical Engineering Department, [§]Materials Science & Engineering, [∥]Applied Physics Program, and [⊥]University of Michigan Energy Institute, University of Michigan, 2250 G.G. Brown Laboratory, 2350 Hayward Street, Ann Arbor, Michigan 48109-2125, United States

Supporting Information

ABSTRACT: The high surface areas and tunable properties of metal−organic frameworks (MOFs) make them attractive materials for applications in catalysis and the capture, storage, and separation of gases. Nevertheless, the limited stability of some MOFs under humid conditions remains a point of concern. Understanding the atomic-scale mechanisms associated with MOF hydrolysis will aid in the design of new compounds that are stable against water and other reactive species. Toward revealing these mechanisms, the present study employs van der Waals-augmented density functional theory, transition-state finding techniques, and thermodynamic integration to predict the thermodynamics and kinetics of water adsorption/insertion into the prototype compound, MOF-5. Adsorption and insertion energetics were evaluated as a function of water coverage, while accounting for the full periodicity of the MOF-5 crystal structure, that is, without resorting to cluster approximations or structural simplifications. The calculations suggest that the thermodynamics of MOF hydrolysis are coverage-dependent: water insertion into the framework becomes exothermic only after a sufficient number of H_2O molecules are coadsorbed in close proximity on a Zn−O cluster. Above this coverage threshold, the adsorbed water clusters facilitate facile water insertion via breaking of Zn−O bonds: the calculated free-energy barrier for insertion is very low, 0.17 eV at 0 K and 0.04 eV at 300 K. Our calculations provide a highly realistic description of the mechanisms underlying the hydrolysis of MOFs under humid working conditions.

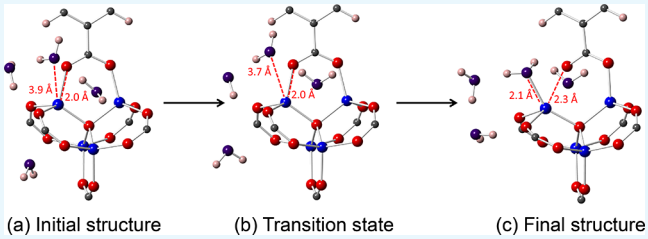

INTRODUCTION

Metal−organic frameworks (MOFs) are crystalline, microporous compounds with potential applications involving adsorption (i.e., gas storage, capture, and separation) and catalysis.[1−4] MOFs hold the record for their specific surface area,[5] and their structure and composition can be varied extensively, resulting in many thousands of known[6] and hypothetical MOFs[7] with a wide range of properties.

Despite this promise, several MOFs are known to exhibit limited stability to humidity,[8−18] which would restrict their use in applications such as CO_2 capture from flue gas or in contexts where exposure to air is likely. For example, Chanut et al.[16] examined CO_2 adsorption in the presence of humidity across a wide range of MOFs using thermogravimetry. Most MOFs exhibited at least a 10% reduction in CO_2 uptake in the presence of water. Similarly, Zuluaga and co-workers[17] reported on the stability of MOF-74 in humid environments and on how this stability impacts CO_2 capture. It was shown that CO_2 uptake is reduced because of the presence of hydroxyl groups formed from the dissociation of water. The hydroxyl attaches to the coordinatively unsaturated metal sites, thereby blocking CO_2 adsorption on these favorable sites.

Perhaps the best-known example of water stability issues in MOFs occurs in the prototype compound MOF-5, which has attracted considerable attention as a gas storage material because of its high storage densities.[6,19−22] The degradation of MOF-5 following exposure to humid air has been reported in several studies.[11,23−28] For example, Long and co-workers reported on the hydrolysis of MOF-5 by measuring the X-ray diffraction spectrum and the hydrogen uptake isotherm of a sample before and after exposure to air.[23] Schröck and co-workers identified the water loading threshold for the degradation of MOF-5; irreversible decomposition was observed after an uptake of 8 wt % water.[29] Cychosz and Matzger analyzed the structure of several MOFs following exposure to dimethylformamide (2 mL) solutions containing 50 to 2000 μL of water; they concluded that the MOF stability was related to the composition and geometry of the metal cluster of MOFs.[30]

Experiments conducted by the present authors observed a sudden increase in water uptake (type V isotherm) in MOF-5—coinciding with a rapid, irreversible structure change—upon exposure to air with a relative humidity of 50% or higher.[31] Below this threshold, water uptake was limited and little structure change was observed for exposure times lasting up to several hours. The faster rates of decomposition observed

Received: August 3, 2017
Accepted: August 11, 2017
Published: August 24, 2017

DOI: 10.1021/acsomega.7b01129
ACS Omega 2017, 2, 4921−4928

at higher humidity levels suggest that the (local) water coverage within the MOF may influence the energetics associated with its irreversible hydrolysis.

Although the limited stability of MOF-5 with respect to water is now well-established,[8,11,23−31] the reaction mechanisms associated with water-induced degradation have been difficult to uncover. To assist in identifying these mechanisms, a small number of studies have employed (classical) molecular dynamics (MD) and first-principles calculations to characterize the atomic-scale features of this process. Greathouse and Allendorf performed one of the earliest MD studies of the water/MOF-5 system.[32] Using a semiempirical force field, they revealed that adsorbed water interacts more strongly with Zn sites than with the carboxylate linker, and that water molecules can insert into MOF-5 upon breaking of Zn−O bonds.[32] Han and co-workers subsequently extended this approach by using the ReaxFF force field.[33] This study proposed a reaction mechanism associated with MOF hydrolysis in which adsorbed water dissociates into a hydroxyl group and a proton. Subsequently, the −OH group bonds to Zn by breaking the Zn−O bond between the metal cluster and the linker. The remaining hydrogen then joins with the organic linker to form carboxylic acid.[33] The ReaxFF force field was also recently used to study the water-induced degradation of various isoreticular MOFs (IRMOFs).[15]

In principle, density functional theory (DFT)-based calculations should provide a highly accurate description of the bond-breaking processes during MOF hydrolysis. However, these calculations remain a challenge because of the large number of atoms in the computational cell (106 atoms in the MOF-5 primitive cell and 424 atoms in the conventional cell). For this reason, cluster approximations[34] or structural simplifications[35−37] are commonly adopted to make the calculations tractable. For example, Low and co-workers used cluster models of several MOFs to examine their hydrothermal stability.[34] More recently, De Toni et al. modeled the effect of water loading on the hydration process in the simplified MOF-5 analogue, IRMOF-0h, in which the benzene ring in the linker was replaced by a linear arrangement of two C atoms.[35] Similarly, Bellarosa et al. studied the formation of water clusters during the degradation process of MOF-5 using a reduced-size primitive cell (1/8 the volume of the conventional unit cell) constructed by adopting higher-symmetry linker orientations.[36] A follow-on study by the same group examined the impact of metal composition on the water stability of IRMOF-1 variants.[37]

Building on these earlier investigations, the present study revisits the reaction mechanism for MOF-5 hydrolysis using DFT calculations. The primary goal is to elucidate the connection between water uptake in MOF-5 and its hydrolysis. This is accomplished by calculating the energetics of water insertion as a function of water coverage. Distinguishing features of our approach are the use of a van der Waals-aware density functional and the full treatment of the MOF crystal structure (i.e., without structural simplifications or cluster model approximations). As a first step, we calculate the thermodynamics of water adsorption at various sites in MOF-5. Subsequently, the energetics for hydrolysis are evaluated as a function of the local coverage of water near the Zn−O insertion point. Water insertion is found to be exothermic only after a critical number of H_2O molecules are adsorbed in close proximity on a given Zn−O cluster. This finding corroborates the experimental observations of an induction period—presumably associated with the nucleation of small, adsorbed water clusters—preceding hydrolysis.[31,38] Finally, the reaction pathway for water insertion into the framework was evaluated at two temperatures using two approaches: at 0 K with the nudged elastic band (NEB) method and at 300 K using thermodynamic integration (TI). In both cases, the presence of explicit, adsorbed water molecules was accounted for. For coverages where insertion is thermodynamically favorable, the barrier for insertion is predicted to be very low, 0.17 eV at 0 K and only 0.04 eV at 300 K. Such a small barrier indicates the likelihood for rapid hydrolysis at moderate humidity levels, in agreement with prior experiments.[31]

RESULTS AND DISCUSSION

Adsorption of Isolated Water Molecules. Figure 1a shows the conventional unit cell of MOF-5. The crystal structure consists of benzenedicarboxylate linkers and Zn_4O metal−oxygen clusters, with these clusters also commonly referred to as secondary building units (SBUs). Five distinct sites were explored for water adsorption. These sites are illustrated as large purple spheres in Figure 1b and labeled with the Greek letters α, β, γ, δ, and ε. The positions of the sites examined are similar to those described in prior experiments[39] and simulations[40] for the adsorption of Ar, N_2, and H_2 in MOF-5. To our knowledge, a detailed sampling of the potential energy surface for H_2O adsorption on MOF-5 has not been

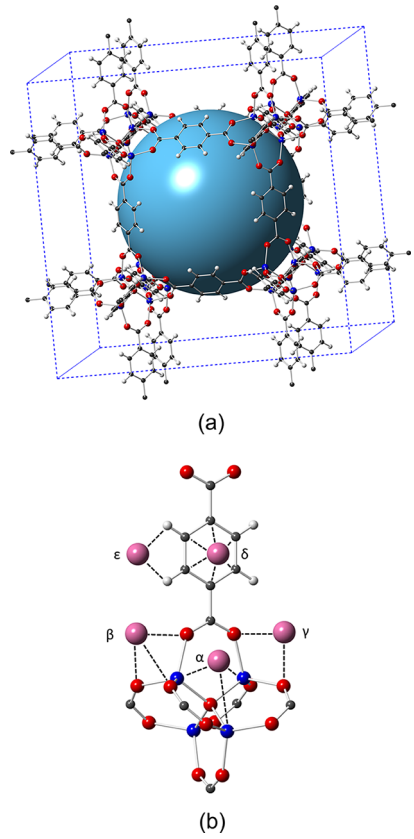

Figure 1. (a) Conventional unit cell of MOF-5. The red spheres represent oxygen, the blue spheres represent Zn, the gray spheres represent C, and the white spheres represent H. (b) Magnification of the metal cluster and the organic linker from panel (a). The purple spheres represent five distinct sites for water adsorption and are labeled with Greek symbols.

DOI: 10.1021/acsomega.7b01129
ACS Omega 2017, 2, 4921−4928

reported. The three sites α, β, and γ refer to the sites on the Zn−O cluster, whereas δ and ε refer to the sites on the benzene ring in the linker. Site α is the closest site to the central oxygen in the Zn cluster; this site is also equidistant to three of the Zn atoms bonded to the central oxygen. Site β is closest to one of the four Zn atoms in the cluster and is equidistant to three of the four oxygen atoms bonded to Zn. Site γ is proximate to two oxygen atoms bonded to Zn. On the linker, site δ is centered above the face of the benzene ring. Site ε is positioned at the edge of the benzene, with equal distances to two hydrogen atoms. Table 1 lists the number of each type of site on a single metal cluster or linker. In total, there are 20 adsorption sites on the metal cluster and 12 sites on the linker.

Table 1. Number and Location of Each Type of Adsorption Site Depicted in Figure 1

location	site name	number of sites
Zn−O cluster	α	4
	β	4
	γ	12
linker	δ	6
	ε	6

Figure 2a plots the adsorption energy, E_{ad}, for a single water molecule for each adsorption site as a function of the exchange−correlation functional employed [Perdew−Burke−Ernzerhof (PBE)-generalized gradient approximation (GGA) and a van der Waals-aware density functional (vdW-DF2)]. The vdW-DF2 predicts more exothermic binding energies than does the GGA regardless of the adsorption geometry. This difference is particularly large for the α site, where the binding predicted by the GGA is approximately 0.2 eV weaker. The weaker binding observed for the GGA is consistent with earlier calculations involving CO_2 and CH_4 adsorption in MOFs[41−43] and can be attributed to the lack of van der Waals interactions in this functional. More generally, the range of binding energies predicted by the vdW-DF2 across all sites (~0.23 eV) is significantly wider than that predicted by the GGA; in the latter case, the adsorption energies are clustered around −0.15 eV. This trend has also been observed for the adsorption of small molecules in other MOFs.[41−43] An additional difference between the functionals pertains to the site preference for H_2O adsorption. The α site is predicted to be the most stable site for adsorption by the vdW-DF2, whereas the GGA predicts the β site to be the most favorable. We also note that the present calculations predict an adsorption energy of −0.19 eV at the β site for the GGA functional; this value is in good agreement with the energy (−0.20 eV) predicted by a previous computational study.[36]

Figure 2b−d tabulates the bond distances between the proximal oxygen atom in an adsorbed water molecule and various atoms in the MOF. This is done for the adsorption sites located on the metal cluster (sites α, β, and γ) as a function of the exchange−correlation functional. In all cases, the bond lengths are greater than 3 Å, consistent with a weak, physisorption interaction. Distances predicted by the vdW-DF2 are systematically shorter than those from the GGA; this is expected, given the larger adsorption energies obtained with the vdW-DF2, Figure 2a.

Another recent computational study of water adsorption in a simplified model of MOF-5 (IRMOF-0h) found a much shorter O(water)−Zn distance of 2.0 Å.[35] The data shown in Figure 2b−d suggest that the shorter distances found in that study are likely an artifact of the structural simplifications employed there; in IRMOF-0h, every benzene in the linker is replaced by two carbon atoms. By removing the bulky benzene rings, it is conceivable that the water molecules can gain closer access to the Zn_4O metal cluster. This assertion was verified by performing adsorption calculations on IRMOF-0h. Indeed,

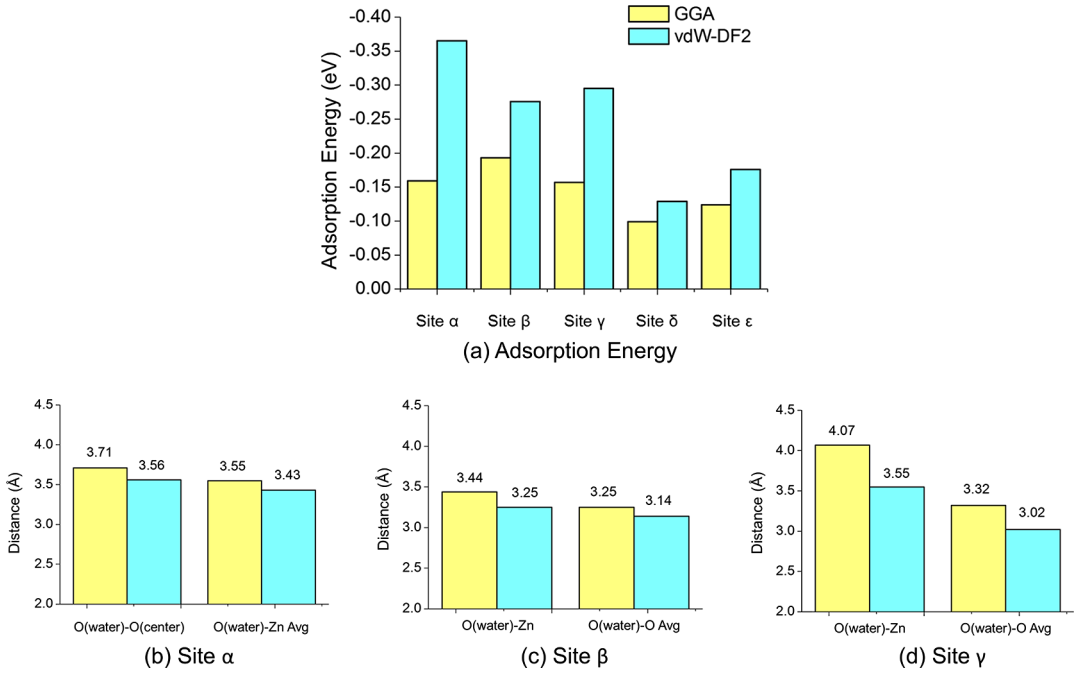

Figure 2. (a) Calculated adsorption energies for water as a function of exchange−correlation functional and adsorption site in MOF-5. (b−d) Calculated distance from proximal O in an adsorbed water molecule to various atoms in MOF-5 for the adsorption sites located on the metal cluster (sites α, β, and γ).

DOI: 10.1021/acsomega.7b01129
ACS Omega 2017, 2, 4921−4928

water was observed to adsorb in this structure with much shorter bond distances of 2.57 Å. Additional comparisons with the IRMOF-0h structure used in ref 35 are provided in Figure S2 in the Supporting Information.

Adsorption of Multiple Water Molecules. In reality, multiple water molecules can adsorb simultaneously on MOF-5 upon exposure to humid air. According to our previous study,[31] the saturation water loading in MOF-5 is ∼13 wt % when exposed to air with a relative humidity exceeding 50%. Assuming that all water molecules preferentially fill the most energetically favorable adsorption sites (α, β, and γ sites residing on the Zn−O cluster), this loading corresponds to the adsorption of approximately five water molecules per metal cluster. We aim to determine the dependence of water adsorption energies on the Zn−O cluster as a function of coverage and adsorption geometry. To accomplish this, multiple water molecules were placed at α, β, and γ sites on the same Zn−O cluster. Coverages of 1−4 molecules were examined. We adopt a naming scheme in which the number and identity of the filled sites specify the coverage and adsorbed configuration. For example, the configuration identified as "$\alpha\alpha$" contains two water molecules adsorbed on α sites. Similarly, "$\alpha\beta\gamma$" corresponds to a configuration where three water molecules are adsorbed in α, β, and γ sites simultaneously. Given the large number (∼1300) of possible configurations for even a small number of adsorbed molecules (4) on a single Zn−O cluster, a systematic enumeration of all configurations was not attempted. Rather, a subset of configurations in which the adsorbed molecules were clustered (i.e., adsorbed at predominantly adjacent sites) was explored. Our preference for these configurations is based on the expectation that water−water interactions are energetically favorable at higher coverages.[36]

From Figure 1a, we observe that site α has the lowest adsorption energy for a single water molecule. If water molecules interact weakly, then we expect that only α sites will be filled, as these sites are well-separated. Figure 3 compares the total adsorption energies for the lowest energy adsorbed configurations identified by our search to configurations in which only α sites are filled. For the highest loading considered, four water molecules, the total adsorption energy assuming that only α sites are occupied is −1.14 eV. For this $\alpha\alpha\alpha\alpha$ configuration, the distance between adjacent H_2O molecules is large, 5.74 Å, signaling that H_2O-H_2O interactions are likely weak. By contrast, a configuration in which H_2O is adsorbed with the configuration $\alpha\alpha\beta\gamma$ yields a more exothermic adsorption energy of −1.40 eV. In this case, the water cluster adopts a more compact arrangement, with H_2O-H_2O distances given by 2.86 Å ($\alpha-\beta$); 4.83 Å ($\alpha-\gamma$); and 2.97 Å ($\beta-\gamma$). A similar trend holds for loadings of two and three molecules: adsorption is preferred in configurations that involve nearby $\alpha\gamma$ and $\gamma\gamma\gamma$ sites (on average, the $\gamma-\gamma$ distance is 2.9 Å). As anticipated, these data suggest that water−water interactions play an important role during the adsorption process: the incoming water molecules preferentially adsorb at adjacent sites rather than filling only the widely separated α sites. This tendency is consistent with the type V isotherm measured in our previous study of water uptake in MOF-5;[31] such an isotherm indicates the presence of sizeable water−water interactions.

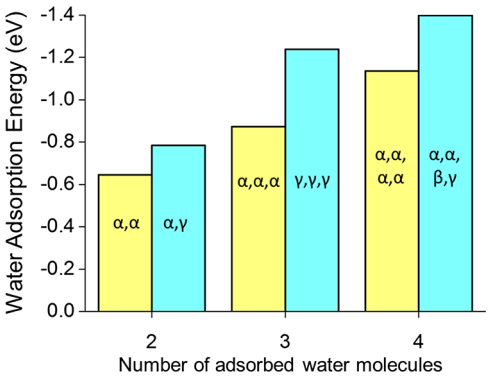

Figure 3. Calculated total adsorption energy for water on a single Zn_4O SBU as a function of coverage and adsorption configuration. For each coverage, the yellow bars (left) represent the adsorption energy in the case where water molecules are widely separated by filling only the α sites. (α sites were previously identified as the most favorable sites for the adsorption of isolated H_2O molecules.) The blue bars (right) represent the adsorption energy for the most energetically favorable water distribution identified amongst many candidate adsorbed geometries. Adsorption geometries are labeled inside each bar.

Thermodynamics of Water Insertion. Having determined the geometries and adsorption energies for small water clusters in MOF-5, we next examine the energetics of water insertion into the framework as a function of water coverage. Prior experiments indicate that the hydrolysis of MOF-5 occurs more rapidly at higher water loadings and is preceded by an induction period, presumably owing to the nucleation of small water clusters.[31,36,38] The exothermicity for water insertion was assessed by evaluating the insertion energy: $\Delta E = E_{final} - E_{initial}$. In this expression, $E_{initial}$ corresponds to a low-energy configuration of n adsorbed water molecules on a given metal cluster, as previously described, and E_{final} represents the energy of a related structure in which one of the adsorbed molecules is inserted as a molecular unit into the MOF by breaking a Zn−O bond. Water insertion will be favorable if $\Delta E < 0$. Several configurations were considered as candidates for the final (inserted) geometry, including various displacements and twists of the linker following the Zn−O bond scission. ΔE was calculated for coverages ranging from 1 to 4 water molecules.

In addition to the reactions where water was inserted as a molecular unit, the energetics of dissociative water insertion were also examined. In the latter scenario, relaxed structures were generated in which the Zn−O bond present in MOF-5 was broken and replaced by Zn−OH(water) and O−H(water) bonds. However, the energy of these hypothetical structures was found to be much higher (∼1 eV) than that of the initial, adsorbed water cluster, indicating that water dissociation is not energetically favorable in this configuration. This is consistent with the findings of ref 36, which reported that dissociative insertion was endothermic by 0.8 eV relative to a metastable physisorbed state.

The insertion energy for (molecular) water into MOF-5 as a function of coverage is shown in Figure 4. With only one molecule adsorbed, water insertion is endothermic: $\Delta E = 0.35$ eV. Insertion becomes increasingly less endothermic as the size of the water cluster grows to two or three molecules. Finally, insertion becomes exothermic when the cluster size reaches four molecules, with $\Delta E = -0.16$ eV. The observation that water insertion is exothermic only at higher coverages is roughly consistent with the experimental observations of rapid degradation in MOF-5 upon exposure to air containing relatively high concentrations of water (50% relative humidity

DOI: 10.1021/acsomega.7b01129
ACS Omega 2017, 2, 4921−4928

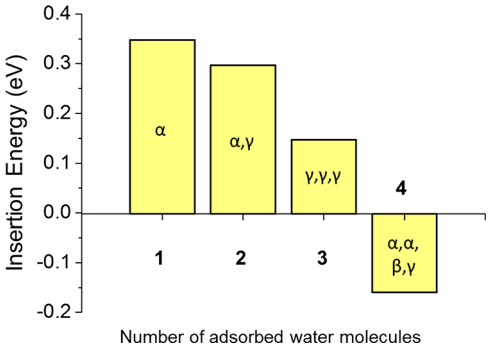

Figure 4. Insertion energy for water into MOF-5 as a function of coverage on a Zn−O cluster. The labels within each bar indicate the configuration of the adsorbed H_2O cluster before insertion.

or higher).[31] As previously described, the water loading determined in those isotherm experiments, equal to 13 wt % or approximately five water molecules per metal cluster, is close to the loading identified here (four molecules) and in an earlier GGA-based study.[31] Although experiments suggest that degradation is most rapid at a loading equivalent to five molecules per cluster, entropic effects could shift some molecules to sites on the linker. Such an effect would bring the predicted computational loading into even better agreement with experiments.

Reaction Pathway at T = 0 K. The reaction pathway for water insertion is illustrated in Figure 5, and the minimum energy pathway for this reaction at T = 0 K (evaluated using the NEB) is plotted in Figure 6a. The initial state for the reaction is shown in Figure 5a, where four water molecules are adsorbed at α, α, β, and γ sites, which is the same low-energy configuration reported in Figure 3. (This configuration is also depicted as the first NEB image/datapoint in Figure 6a, where its energy is assigned a value of zero.) Upon approaching the transition state, shown in Figure 5b and corresponding to NEB image 4 in Figure 6a, the water molecule occupying the β site migrates toward the Zn atom. The energy barrier for this process is relatively small, only 0.17 eV. (The small maximum present at hyperdistance ∼10 Å is likely an artifact of noise in the forces present on the images that span this maximum.) Finally, Figure 5c represents the product state where the water molecules have been inserted into the framework by breaking a Zn−O bond. The inserted molecule forms a new bond of length 2.1 Å between Zn and O(water). The original (and now broken) Zn−O(MOF) bond lengthens to 2.3 Å from its initial value of 2.0 Å. The O(MOF) stranded by water insertion subsequently forms a double bond with its neighboring C, that is, a carbonyl group. Meanwhile, the three adsorbed water molecules remain in close proximity to the inserted molecule, forming a "water chain" with intermolecular H−O distances of 1.7−2.3 Å, Figure 5c. These distances are consistent with the intermolecular H−O bond lengths typical of hydrogen bonding in water, ∼2.0 Å. The formation of such a water chain has also been discussed in prior studies[35,36] and is expected to stabilize the transition and/or hydrolyzed states.

Reaction Pathway at T = 300 K. Figure 6b illustrates the reaction pathway for water insertion at 300 K using TI.[44] Different from the NEB calculation, the TI pathway depicts the variation in *free energy* (i.e., including entropic contributions) during MOF hydrolysis. The pathway was calculated using nine intermediate TI images between the reactant (Figure 5a) and product (Figure 5c) states, with the reaction coordinate ξ taken as the difference $r_1 - r_2$. Here, r_1 represents the Zn−O bond length in MOF-5 (Figure 5a); this bond breaks during the insertion of a H_2O molecule, increasing from 2.0 to 2.3 Å. Similarly, r_2 corresponds to the Zn−O distance between a MOF Zn ion and the oxygen in the inserted water molecule; this distance shrinks from 3.9 to 2.1 Å during water insertion. The reaction pathway is revealed by varying r_1 and r_2 monotonically between the distances described above.

Figure 6a shows that the transition state for water insertion at 300 K occurs for the values of the reaction coordinate ξ between approximately −1.5 and −1.0 Å, corresponding to bond lengths r_1 = 2.06 to 2.15 Å and r_2 = 3.54 to 3.0 Å. The activation energy estimated by TI, 0.04 eV, is comparable to the thermal energy (k_BT) at room temperature, indicating that water insertion will be facile at 300 K. The free-energy barrier is also slightly smaller than that obtained from the (static) 0 K NEB calculation, 0.17 eV. The modest temperature dependence of the activation energy indicates that entropic effects play an important but not overwhelming role in the reaction energetics. Furthermore, we note that the barriers reported here are in qualitative agreement with earlier studies of water insertion in MOF-5 that employed lower levels of theory and simplified structural models. For example, the 0.08 eV barrier reported in ref 35 is bounded by the 0 and 300 K barriers estimated in the present study. Similarly, ab initio molecular dynamics (AIMD) calculations performed by Bellarosa et al.[36] at 300 K revealed that water insertion was barrierless for local coverages of five H_2O molecules, in good agreement with the 0.04 eV barrier

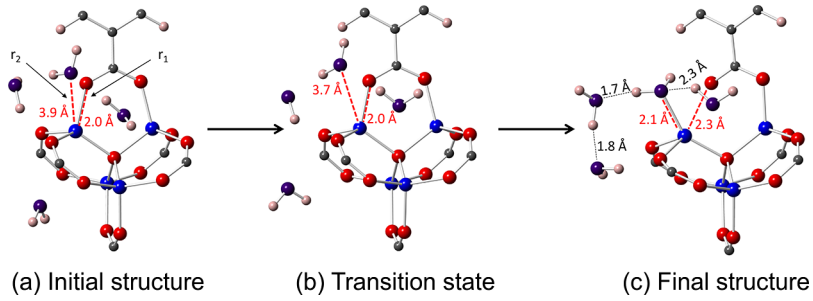

Figure 5. Water insertion process in MOF-5. (a) Magnification of MOF-5 structure with four water molecules adsorbed near the Zn−O cluster. (b) Transition state as determined by the NEB calculations at T = 0 K. (c) Final MOF-5 structure containing a Zn−O bond broken via the insertion of a single water molecule. The color scheme for MOF atoms is the same as in Figure 1b, with the exception that O atoms in the water molecules are purple to distinguish them from oxygen in the MOF (red). Black dashed lines/text indicate hydrogen bond lengths between adjacent water molecules. Red dashed lines/text illustrate Zn−O bond distances. r_1 is the Zn−O(MOF) distance, whereas r_2 is the Zn−O(inserted water) distance.

DOI: 10.1021/acsomega.7b01129
ACS Omega 2017, 2, 4921−4928

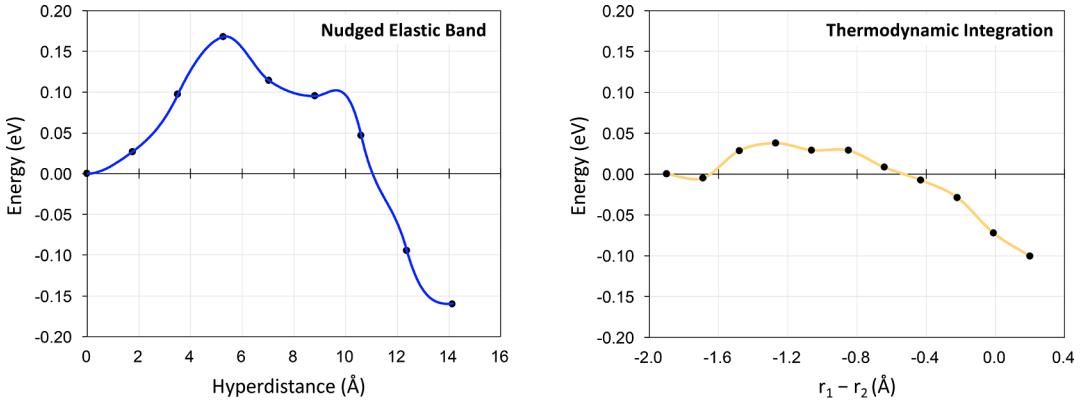

Figure 6. Energy profiles for water insertion into MOF-5 as a function of reaction coordinate at (a) 0 and (b) 300 K. In (a), the static NEB method is used to estimate the 0 K reaction barrier. In (b), the free-energy barrier is evaluated using TI. r_1 and r_2 represent Zn−O distances, as shown in Figure 5.

reported here at the same temperature with TI on a four-molecule adsorbed cluster.

CONCLUSIONS

Enhancing the robustness of MOFs to water and other reactive species remains an important challenge in translating these materials from the laboratory bench to practical applications. Understanding the processes responsible for MOF hydrolysis is a prerequisite for the rational design of new compounds with improved stability. Toward this goal, the present study has examined the energetics associated with water adsorption and insertion into the prototype compound MOF-5 as a function of coverage. Distinguishing features of our study include the use of a van der Waals-aware functional to capture dispersion interactions present during molecular adsorption, evaluation of activation (free) energies for water insertion at 0 and 300 K, and treatment of the full periodic unit cell of MOF-5 without simplifications to the crystal structure.

A comparison of the vdW-DF2 functional with a conventional gradient-corrected functional (PBE-GGA) revealed important qualitative and quantitative differences regarding the energetics and site preference for water adsorption. The vdW-DF2 favors water adsorption on the SBU, rather than on the linker. This differs from the trend predicted by the PBE-GGA, which exhibits a more uniform distribution of adsorption energies on both the linker and SBU.

A key finding of our study is that the thermodynamics of water insertion into MOF-5 is coverage-dependent: insertion becomes thermodynamically favorable only when a critical number of water molecules (four or more) are coadsorbed as relatively compact clusters on the same Zn_4O secondary building unit of the MOF. This observation is in good agreement with experimental measurements, which show that hydrolysis is slow at low water coverages and is preceded by an incubation period; we speculate that the latter process is due to the nucleation and growth of water clusters of sufficient size on a given SBU. Once a sufficient coverage has been achieved, the insertion of molecular water into the Zn−O bonds proceeds with a very low free-energy activation barrier, 0.04 eV at 300 K, consistent with a rapid hydrolysis reaction under ambient temperatures.

Our calculations lend further support to the notion that the rate of MOF degradation depends strongly on the operating environment. Although it is now clear that some MOFs are unstable to hydrolysis in an absolute sense, under low-to-moderate humidity conditions, the rate of hydrolysis can be slow enough to allow exposure for several days without significant degradation. Efforts to expand this "stability window" to higher temperatures and humidity levels will benefit from the mechanistic understanding provided by this study.

COMPUTATIONAL METHODS

Water adsorption and insertion calculations were performed using density functional theory[45] [Vienna ab initio simulation package (VASP)[46,47] code]. Calculations were performed using conventional gradient-corrected functionals (PBE-GGA)[48] and with the vdW-DF2[49] van der Waals-augmented functional. The MOF-5 crystal structure was adopted from diffraction experiments.[50] The full 3D periodic crystal structure based on the 106-atom MOF-5 primitive cell was used without cluster approximations or other structural simplifications.[34−37] All calculations were performed with a plane-wave energy cutoff energy of 500 eV; the Brillouin zone was sampled at the Γ-point. Interactions between the core and valence electrons were described using the projector augmented-wave method[47] with valence electron configurations as follows: Zn: $3d^{10}4s^2$; O: $2s^22p^4$; and C: $2s^22p^2$.

The water-free MOF-5 structure was optimized separately using the PBE-GGA functional and vdW-DF2 by minimizing the atomic forces and stresses on the cell with respect to the cell shape, volume, and atom positions. The lattice parameters obtained following these relaxations, 26.12 Å (PBE-GGA) and 26.35 Å (vdW-DF2), are in reasonable agreement with the experimental values (25.67−25.89 Å).[51]

To identify the favorable locations for water adsorption, a single water molecule was placed at several candidate adsorption sites; for each configuration, all atomic degrees of freedom were relaxed while keeping the cell shape and volume fixed at the value obtained from the relaxation of the water-free structure using the same functional (GGA or vdW-DF2). The adsorption energy was calculated according to the equation

$$E_{ad} = E_{MOF\text{-}5,water} - E_{MOF\text{-}5} - nE_{water} \quad (1)$$

Here, $E_{MOF\text{-}5,water}$ refers to the energy for MOF-5 with n adsorbed water molecules, $E_{MOF\text{-}5}$ is the energy of the water-free

DOI: 10.1021/acsomega.7b01129
ACS Omega 2017, 2, 4921−4928

MOF-5 cell, and E_{water} is the energy of an isolated water molecule calculated using a orthorhombic simulation cell with dimensions of 10 × 11 × 12 Å.

The climbing image NEB method[52,53] was used to calculate the activation energy for water insertion into MOF-5 at 0 K. Seven NEB images were used to evaluate the minimum energy reaction pathway between the reactant (i.e., adsorbed water) and product (i.e., inserted water) states.

In addition to evaluating the activation energy at 0 K, the free-energy barrier at T = 300 K was determined using TI.[44] In TI, the change in free energy between the reactant (R) and product (P) states, $\Delta A_{R\rightarrow P}$, is given by a path integral along a reaction coordinate ξ connecting those states

$$\Delta A_{R\rightarrow P} = \int_{\xi_R}^{\xi_P} \left(\frac{\partial A}{\partial \xi}\right)_{\xi^*} d\xi \quad (2)$$

The free-energy gradient, $\left(\frac{\partial A}{\partial \xi}\right)$, is obtained from a series of constrained AIMD simulations.[44,54] AIMD was performed in the canonical ensemble (NVT) at T = 300 K with an Andersen thermostat[44,55] at a collision rate of 0.05 fs^{-1}.[56] The reaction path was composed of nine intermediate configurations between the R and P states. Constrained AIMD was performed for 6 ps on each of these 11 configurations with a time step of 1 fs. The last 4 ps of each trajectory was used to calculate the parameters for TI.

■ ASSOCIATED CONTENT

Supporting Information

The Supporting Information is available free of charge on the ACS Publications website at DOI: 10.1021/acsomega.7b01129.

Comparison of water adsorption distances to metal cluster atoms in MOF-5 and IRMOF-0h; variation of r_1 and r_2 for NEB and TI methods; example VASP input files; relaxed adsorption configurations; and relaxed configurations for water insertion (PDF)

■ AUTHOR INFORMATION

Corresponding Author

*E-mail: djsiege@umich.edu. Phone: 734-764-4808 (D.J.S.).

ORCID

Donald J. Siegel: 0000-0001-7913-2513

Present Address

#Ford Motor Company, 1201 Village Road, Fuel Cell Center, Dearborn, MI 48121.

Notes

The authors declare no competing financial interest.

■ ACKNOWLEDGMENTS

Funding for this study was provided by the U.S. Department of Energy, Office of Energy Efficiency and Renewable Energy, award number DE-FC36-GO19002. Y.M. acknowledges helpful discussions with Max Radin, Malay Rana, Hyun Koh, and Sheng Yang. N.K. acknowledges helpful discussions with T. Bucko.

■ REFERENCES

(1) Mueller, U.; Schubert, M.; Teich, F.; Puetter, H.; Schierle-Arndt, K.; Pastré, J. Metal−organic frameworks—prospective industrial applications. *J. Mater. Chem.* **2006**, *16*, 626−636.

(2) Schlichte, K.; Kratzke, T.; Kaskel, S. Improved synthesis, thermal stability and catalytic properties of the metal-organic framework compound CU3(BTC)(2). *Microporous Mesoporous Mater.* **2004**, *73*, 81−88.

(3) Yaghi, O. M.; O'Keeffe, M.; Ockwig, N. W.; Chae, H. K.; Eddaoudi, M.; Kim, J. Reticular synthesis and the design of new materials. *Nature* **2003**, *423*, 705−714.

(4) Rowsell, J. L. C.; Yaghi, O. M. Metal−organic frameworks: a new class of porous materials. *Microporous Mesoporous Mater.* **2004**, *73*, 3−14.

(5) Kayalvizhi, M.; Berchmans, L. J. Combustion Synthesis of Lanthanum Substituted $LiNiO_2$ Using Hexamine as a Fuel. *E-J. Chem.* **2010**, *7*, S137−S142.

(6) Goldsmith, J.; Wong-Foy, A. G.; Cafarella, M. J.; Siegel, D. J. Theoretical Limits of Hydrogen Storage in Metal−Organic Frameworks: Opportunities and Trade-Offs. *Chem. Mater.* **2013**, *25*, 3373−3382.

(7) Wilmer, C. E.; Leaf, M.; Lee, C. Y.; Farha, O. K.; Hauser, B. G.; Hupp, J. T.; Snurr, R. Q. Large-scale screening of hypothetical metal-organic frameworks. *Nat. Chem.* **2011**, *4*, 83−89.

(8) Burtch, N. C.; Jasuja, H.; Walton, K. S. Water stability and adsorption in metal−organic frameworks. *Chem. Rev.* **2014**, *114*, 10575−10612.

(9) Gul-E-Noor, F.; Jee, B.; Pöppl, A.; Hartmann, M.; Himsl, D.; Bertmer, M. Effects of varying water adsorption on a Cu3(BTC)2 metal−organic framework (MOF) as studied by ^1H and ^{13}C solid-state NMR spectroscopy. *Phys. Chem. Chem. Phys.* **2011**, *13*, 7783−7788.

(10) Gul-E-Noor, F.; Michel, D.; Krautscheid, H.; Haase, J.; Bertmer, M. Time dependent water uptake in Cu3(btc)2 MOF: Identification of different water adsorption states by 1H MAS NMR. *Microporous Mesoporous Mater.* **2013**, *180*, 8−13.

(11) Liang, Z.; Marshall, M.; Chaffee, A. L. CO_2 adsorption, selectivity and water tolerance of pillared-layer metal organic frameworks. *Microporous Mesoporous Mater.* **2010**, *132*, 305−310.

(12) Jasuja, H.; Huang, Y.-g.; Walton, K. S. Adjusting the stability of metal−organic frameworks under humid conditions by ligand functionalization. *Langmuir* **2012**, *28*, 16874−16880.

(13) DeCoste, J. B.; Peterson, G. W.; Jasuja, H.; Glover, T. G.; Huang, Y.-g.; Walton, K. S. Stability and degradation mechanisms of metal−organic frameworks containing the Zr6O4(OH)(4) secondary building unit. *J. Mater. Chem. A* **2013**, *1*, 5642−5650.

(14) Masala, A.; Vitillo, J. G.; Mondino, G.; Grande, C. A.; Blom, R.; Manzoli, M.; Marshall, M.; Bordiga, S. CO_2 Capture in Dry and Wet Conditions in UTSA-16 Metal−Organic Framework. *ACS Appl. Mater. Interfaces* **2017**, *9*, 455−463.

(15) Liu, X. Y.; Pai, S. J.; Han, S. S. ReaxFF Molecular Dynamics Simulations of Water Stability of Interpenetrated Metal−Organic Frameworks. *J. Phys. Chem. C* **2017**, *121*, 7312−7318.

(16) Chanut, N.; Bourrelly, S.; Kuchta, B.; Serre, C.; Chang, J.-s.; Wright, P. A.; Llewellyn, P. L. Screening the Effect of Water Vapour on Gas Adsorption Performance: Application to CO2 Capture from Flue Gas in Metal-Organic Frameworks. *ChemSusChem* **2017**, *10*, 1543−1553.

(17) Zuluaga, S.; Fuentes-Fernandez, E. M. A.; Tan, K.; Xu, F.; Li, J.; Chabal, Y. J.; Thonhauser, T. Understanding and controlling water stability of MOF-74. *J. Mater. Chem. A* **2016**, *4*, 5176−5183.

(18) Ding, N.; Li, H.; Feng, X.; Wang, Q.; Wang, S.; Ma, L.; Zhou, J.; Wang, B. Partitioning MOF-5 into Confined and Hydrophobic Compartments for Carbon Capture under Humid Conditions. *J. Am. Chem. Soc.* **2016**, *138*, 10100−10103.

(19) Ming, Y.; Purewal, J.; Liu, D.; Sudik, A.; Xu, C.; Yang, J.; Veenstra, M.; Rhodes, K.; Soltis, R.; Warner, J.; Gaab, M.; Müller, U.; Siegel, D. J. Thermophysical properties of MOF-5 powders. *Microporous Mesoporous Mater.* **2014**, *185*, 235−244.

(20) Purewal, J. J.; Liu, D.; Yang, J.; Sudik, A.; Siegel, D. J.; Maurer, S.; Müller, U. Increased volumetric hydrogen uptake of MOF-5 by powder densification. *Int. J. Hydrogen Energy* **2012**, *37*, 2723−2727.

DOI: 10.1021/acsomega.7b01129
ACS Omega 2017, 2, 4921−4928

(21) Liu, D.; Purewal, J. J.; Yang, J.; Sudik, A.; Maurer, S.; Mueller, U.; Ni, J.; Siegel, D. J. MOF-5 composites exhibiting improved thermal conductivity. *Int. J. Hydrogen Energy* **2012**, *37*, 6109−6117.
(22) Ming, Y.; Chi, H.; Blaser, R.; Xu, C.; Yang, J.; Veenstra, M.; Gaab, M.; Müller, U.; Uher, C.; Siegel, D. J. Anisotropic thermal transport in MOF-5 composites. *Int. J. Heat Mass Transfer* **2015**, *82*, 250−258.
(23) Kaye, S. S.; Dailly, A.; Yaghi, O. M.; Long, J. R. Impact of preparation and handling on the hydrogen storage properties of Zn_4O(1,4-benzenedicarboxylate)3 (MOF-5). *J. Am. Chem. Soc.* **2007**, *129*, 14176−14177.
(24) Huang, L.; Wang, H.; Chen, J.; Wang, Z.; Sun, J.; Zhao, D.; Yan, Y. Synthesis, morphology control, and properties of porous metal−organic coordination polymers. *Microporous Mesoporous Mater.* **2003**, *58*, 105−114.
(25) Hausdorf, S.; Wagler, J.; Mo*β*ig, R.; Mertens, F. O. R. L. Proton and water activity-controlled structure formation in zinc carboxylate-based metal organic frameworks. *J. Phys. Chem. A* **2008**, *112*, 7567−7576.
(26) Han, S.; Huang, Y.; Watanabe, T.; Nair, S.; Walton, K. S.; Sholl, D. S.; Meredith, J. C. MOF stability and gas adsorption as a function of exposure to water, humid air, SO_2, and NO_2. *Microporous Mesoporous Mater.* **2013**, *173*, 86−91.
(27) Jasuja, H.; Burtch, N. C.; Huang, Y.-g.; Cai, Y.; Walton, K. S. Kinetic water stability of an isostructural family of zinc-based pillared metal−organic frameworks. *Langmuir* **2013**, *29*, 633−642.
(28) Paranthaman, S.; Coudert, F.-X.; Fuchs, A. H. Water adsorption in hydrophobic MOF channels. *Phys. Chem. Chem. Phys.* **2010**, *12*, 8123−8129.
(29) Schröck, K.; Schröder, F.; Heyden, M.; Fischer, R. A.; Havenith, M. Characterization of interfacial water in MOF-5 (Zn4(O)(BDC)-3)—a combined spectroscopic and theoretical study. *Phys. Chem. Chem. Phys.* **2008**, *10*, 4732−4739.
(30) Cychosz, K. A.; Matzger, A. J. Water stability of microporous coordination polymers and the adsorption of pharmaceuticals from water. *Langmuir* **2010**, *26*, 17198−17202.
(31) Ming, Y.; Purewal, J.; Yang, J.; Xu, C.; Soltis, R.; Warner, J.; Veenstra, M.; Gaab, M.; Müller, U.; Siegel, D. J. Kinetic Stability of MOF-5 in Humid Environments: Impact of Powder Densification, Humidity Level, and Exposure Time. *Langmuir* **2015**, *31*, 4988−4995.
(32) Greathouse, J. A.; Allendorf, M. D. The interaction of water with MOF-5 simulated by molecular dynamics. *J. Am. Chem. Soc.* **2006**, *128*, 10678−10679.
(33) Han, S. S.; Choi, S.-H.; van Duin, A. C. T. Molecular dynamics simulations of stability of metal−organic frameworks against H2O using the ReaxFF reactive force field. *Chem. Commun.* **2010**, *46*, 5713−5715.
(34) Low, J. J.; Benin, A. I.; Jakubczak, P.; Abrahamian, J. F.; Faheem, S. A.; Willis, R. R. Virtual high throughput screening confirmed experimentally: porous coordination polymer hydration. *J. Am. Chem. Soc.* **2009**, *131*, 15834−15842.
(35) De Toni, M.; Jonchiere, R.; Pullumbi, P.; Coudert, F.-X.; Fuchs, A. H. How can a hydrophobic MOF be water-unstable? Insight into the hydration mechanism of IRMOFs. *ChemPhysChem* **2012**, *13*, 3497−3503.
(36) Bellarosa, L.; Castillo, J. M.; Vlugt, T.; Calero, S.; López, N. On the Mechanism Behind the Instability of Isoreticular Metal−Organic Frameworks (IRMOFs) in Humid Environments. *Chem.—Eur. J.* **2012**, *18*, 12260−12266.
(37) Bellarosa, L.; Calero, S.; López, N. Early stages in the degradation of metal−organic frameworks in liquid water from first-principles molecular dynamics. *Phys. Chem. Chem. Phys.* **2012**, *14*, 7240−7245.
(38) Guo, P.; Dutta, D.; Wong-Foy, A. G.; Gidley, D. W.; Matzger, A. J. Water sensitivity in Zn4O-based MOFs is structure and history dependent. *J. Am. Chem. Soc.* **2015**, *137*, 2651−2657.
(39) Rowsell, J. L. C.; Spencer, E. C.; Eckert, J.; Howard, J. A. K.; Yaghi, O. M. Gas adsorption sites in a large-pore metal-organic framework. *Science* **2005**, *309*, 1350−1354.
(40) Mueller, T.; Ceder, G. A density functional theory study of hydrogen adsorption in MOF-5. *J. Phys. Chem. B* **2005**, *109*, 17974−17983.
(41) Rana, M. K.; Koh, H. S.; Hwang, J.; Siegel, D. J. Comparing van der Waals Density Functionals for CO2 Adsorption in Metal Organic Frameworks. *J. Phys. Chem. C* **2012**, *116*, 16957−16968.
(42) Rana, M. K.; Koh, H. S.; Zuberi, H.; Siegel, D. J. Methane Storage in Metal-Substituted Metal−Organic Frameworks: Thermodynamics, Usable Capacity, and the Impact of Enhanced Binding Sites. *J. Phys. Chem. C* **2014**, *118*, 2929−2942.
(43) Koh, H. S.; Rana, M. K.; Hwang, J.; Siegel, D. J. Thermodynamic screening of metal-substituted MOFs for carbon capture. *Phys. Chem. Chem. Phys.* **2013**, *15*, 4573−4581.
(44) Bucko, T. Ab initio calculations of free-energy reaction barriers. *J. Phys.: Condens. Matter* **2008**, *20*, 064211.
(45) Hohenberg, P.; Kohn, W. Inhomogeneous Electron Gas. *Phys. Rev. B: Condens. Matter Mater. Phys.* **1964**, *136*, B864−B871.
(46) Kresse, G.; Furthmüller, J. Efficient iterative schemes for ab initio total-energy calculations using a plane-wave basis set. *Phys. Rev. B: Condens. Matter Mater. Phys.* **1996**, *54*, 11169−11186.
(47) Blöchl, P. E. Projector augmented-wave method. *Phys. Rev. B: Condens. Matter Mater. Phys.* **1994**, *50*, 17953−17979.
(48) Perdew, J. P.; Burke, K.; Ernzerhof, M. Generalized gradient approximation made simple. *Phys. Rev. Lett.* **1996**, *77*, 3865−3868.
(49) Dion, M.; Rydberg, H.; Schröder, E.; Langreth, D. C.; Lundqvist, B. I. Van der Waals Density Functional for General Geometries. *Phys. Rev. Lett.* **2004**, *92*, 246401.
(50) Rosi, N. L.; Eckert, J.; Eddaoudi, M.; Vodak, D. T.; Kim, J.; O'Keeffe, M.; Yaghi, O. M. Hydrogen storage in microporous metal-organic frameworks. *Science* **2003**, *300*, 1127−1129.
(51) Eddaoudi, M.; Kim, J.; Rosi, N.; Vodak, D.; Wachter, J.; O'Keeffe, M.; Yaghi, O. M. Systematic design of pore size and functionality in isoreticular MOFs and their application in methane storage. *Science* **2002**, *295*, 469−472.
(52) Henkelman, G.; Jónsson, H. Improved tangent estimate in the nudged elastic band method for finding minimum energy paths and saddle points. *J. Chem. Phys.* **2000**, *113*, 9978−9985.
(53) Henkelman, G.; Uberuaga, B. P.; Jónsson, H. A climbing image nudged elastic band method for finding saddle points and minimum energy paths. *J. Chem. Phys.* **2000**, *113*, 9901−9904.
(54) Carter, E. A.; Ciccotti, G.; Hynes, J. T.; Kapral, R. Constrained Reaction Coordinate Dynamics for the Simulation of Rare Events. *Chem. Phys. Lett.* **1989**, *156*, 472−477.
(55) Andersen, H. C. Molecular dynamics simulations at constant pressure and/or temperature. *J. Chem. Phys.* **1980**, *72*, 2384−2393.
(56) Groß, A. Ab initio molecular dynamics simulations of the O 2/Pt(1 1 1) interaction. *Catal. Today* **2016**, *260*, 60−65.

DOI: 10.1021/acsomega.7b01129
ACS Omega 2017, 2, 4921−4928